

Numerical simulation of seismic tests on precast concrete structures with various arrangements of cladding panels

Bruno Dal Lago*

Department of Civil and Environmental Engineering, Politecnico di Milano, Piazza Leonardo da Vinci 32, 20133 Milano, Italy

(Received March 11, 2018, Revised February 1, 2019, Accepted February 2, 2019)

Abstract. The unexpected seismic interaction of dry-assembled precast concrete frame structures typical of the European heritage with their precast cladding panels brought to extensive failures of the panels during recent earthquakes due to the inadequateness of their connection systems. Following this recognition, an experimental campaign of cyclic and pseudo-dynamic tests has been performed at ELSA laboratory of the Joint Research Centre of the European Commission on a full-scale prototype of precast structure with vertical and horizontal cladding panels within the framework of the Safecladding project. The panels were connected to the frame structure by means of innovative arrangements of fastening systems including isostatic, integrated and dissipative. Many of the investigated configurations involved a strong frame-cladding interaction, modifying the structural behaviour of the frame turning it into highly non-linear since small deformation. In such cases, properly modelling the connections becomes fundamental in the framework of a design by non-linear dynamic analysis. This paper presents the peculiarities of the numerical models of precast frame structures equipped with the various cladding connection systems which have been set to predict and simulate the experimental results from pseudo-dynamic tests. The comparison allows to validate the structural models and to derive recommendations for a proper modelling of the different types of existing and innovative cladding connection systems.

Keywords: precast structures; cladding panels; earthquake engineering; connection devices; numerical modelling

1. Introduction

Concrete panels are often used to clad structures. They are usually considered as non-structural elements, assuming they do not interact with the structure. However, their connection system rarely allows their complete de-coupling from the motion of the structure (Gjelvik 1973, Palsson *et al.* 1984, Henry and Roll 1986, Baird *et al.* 2012, Biondini *et al.* 2013, Magliulo *et al.* 2014a), as also observed from full-scale experimental tests (Wang 1987, Okazaki *et al.* 2007, Biondini and Toniolo 2009). This issue is pronounced for precast frame structures with hinged beam-to-column connections, due to the high cladding-structure relative displacement demand induced by their flexibility (Fischinger *et al.* 2008, Biondini and Toniolo 2009, Bournas *et al.* 2013a, Negro *et al.* 2013, Brunesi *et al.* 2015a, Babič and Dolšek 2016, Dal Lago *et al.* 2016, 2018e, Buratti *et al.* 2017, Magliulo *et al.* 2018). Post-earthquake field observations showed the inadequacy of traditional cladding panel connection systems to accommodate the seismic drifts of these structures (Ghosh and Cleland 2012, Toniolo and Colombo 2012, Bournas *et al.* 2013b, Magliulo *et al.* 2014b, Belleri *et al.* 2015, Savoia *et al.* 2017, Batalha *et al.* 2019). The issue of cladding-structure interaction in precast structures has been the subject of a 3-years European research project entitled Safecladding. Starting from the

definition of the design and technological framework of the cladding connection system (Biondini *et al.* 2013), the project developed investigations on isostatic (Zoubek *et al.* 2016, 2018, Dal Lago *et al.* 2017b, Dal Lago and Lamperti Tornaghi 2018), dissipative (Dal Lago *et al.* 2017a, 2018b, c, d, Yuksel *et al.* 2018) and integrated (Psycharis *et al.* 2018) connection systems. Full-scale tests on a precast cladded frame assembly were performed, investigating the proposed solutions (Negro and Lamperti Tornaghi 2017, Toniolo and Dal Lago 2017).

Previous testing and analysis on some typical cladding connection systems for precast structures was carried out by Metelli *et al.* (2011), Brunesi *et al.* (2015b) and Belleri *et al.* (2016, 2018). The use of cladding panels to stiffen the structure and dissipate energy was also proposed for precast structures by Scotta *et al.* (2016) with reference to stacked horizontal panels. This concept was developed for multi-storey apartment buildings by Gaiotti and Smith (1992), Pinelli *et al.* (1992, 1993, 1996), Cohen and Powell (1993) and Hobelmann *et al.* (2012). The seismic behaviour of large buildings stiffened by peripheral panels was investigated by Fleischman *et al.* (1998), Belleri *et al.* (2014), Pecce *et al.* (2014), Dal Lago *et al.* (2018a) and Dal Lago and Ferrara (2018).

The proposed solutions for innovative connection systems of cladding panels, experimentally assessed and validated within the Safecladding project, may provide significant modifications of the structural behaviour of the precast frame structures under lateral loading. The structural design of most of these systems, often behaving highly non-linearly since small deformation, may need to be performed

*Corresponding author, Ph.D.
E-mail: brunoalberto.dallago@polimi.it

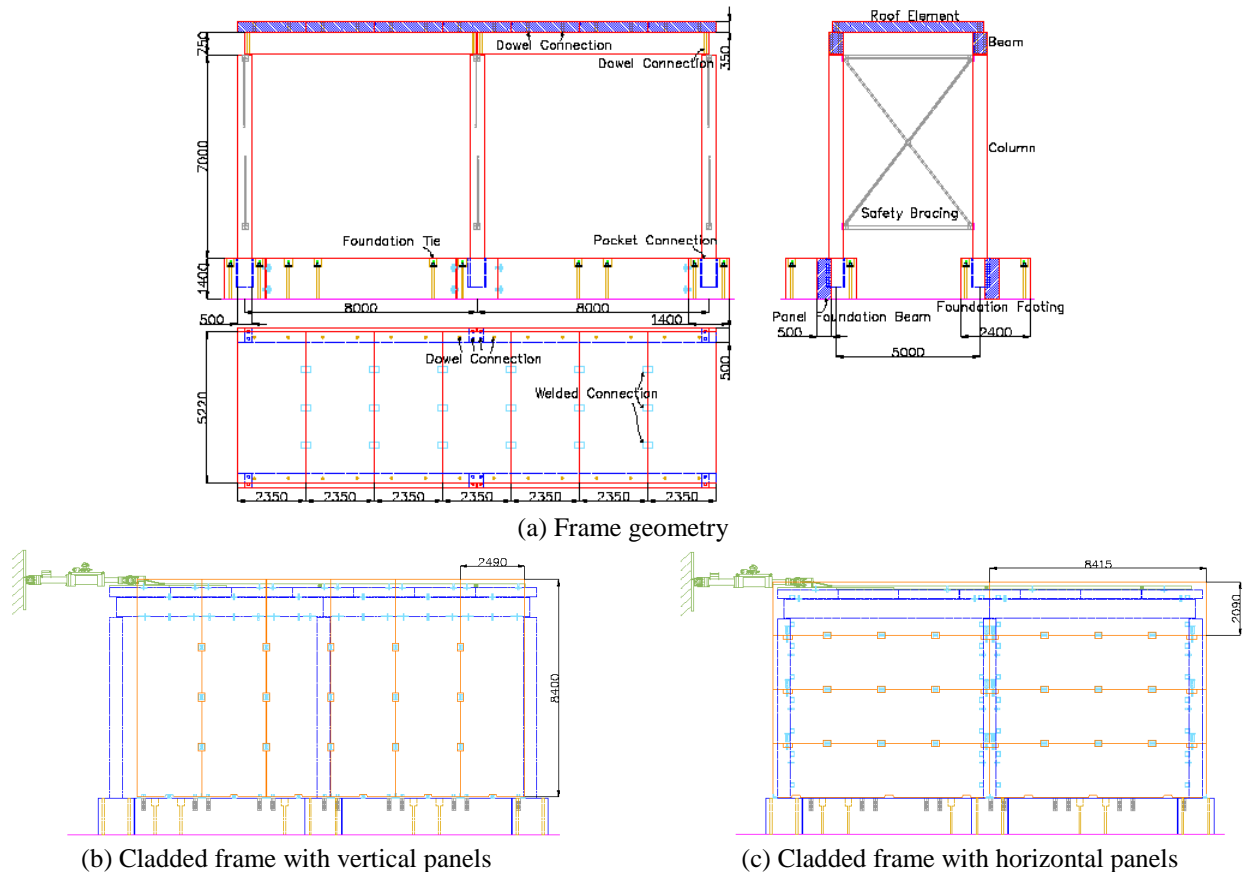


Fig. 1 Full-scale prototype of precast structure

through dynamic non-linear analysis only, due to the difficult framing into traditional structural systems codified in the standards to be designed through equivalent elastic approaches. Innovative simplified seismic design procedures for precast structures were recently assessed by Belleri (2017) and Dal Lago and Molina (2018), however still involving a detailed structural modelling of the assembly.

The cited literature contains information about non-linear modelling of the precast frame structure and of a limited number of bare connection devices, and therefore a designer may face difficulties in setting a proper model. This paper aims at providing information about the detailed structural modelling of precast frame structures with various systems of cladding panels, describing the modelling solutions adopted at Politecnico di Milano to predict the experimental results from pseudo-dynamic seismic tests performed at the ELSA laboratory of the Joint Research Centre of the European Commission on the Safecladding full-scale precast structure prototype. The numerical simulation was used as a fundamental tool to predict the seismic performance of the prototype (forces and displacements) so to avoid its excessive damaging to occur prior to the final tests, and to check the compatibility of the instrumentation. The peculiar modelling described in the paper for structural elements and connections can be used as a reference by the designers willing to employ dynamic non-linear analysis for the seismic design of precast structures with different connection systems of the cladding panels.

2. Full-scale prototype of precast structures with cladding panels

An extensive experimental programme regarding the cyclic and pseudo-dynamic behaviour of a precast building prototype cladded with different panel arrangements has been designed by the research group of Politecnico di Milano and carried out by ELSA/JRC team within the Safecladding project. The specimen has been designed in detail, cast and assembled by Styl-Comp company. The prototype is a dry-assembled single-storey precast frame structure representing a typical industrial building in Southern Europe, with single 5 m wide nave covered by solid concrete panels and 8 m span double bay. Its mass is the same of an equivalent wider building model with a 16 m wide nave covered with TT roof members, representing a typical structural arrangement for the European precast construction industry. Fig. 1(a) shows the geometry of the laboratory prototype frame structure.

The foundations are made with six $2.40 \times 1.40 \times 1.40$ m pocket elements, provided with a central 0.80 m deep void and with running holes for the installation on the strong floor of the laboratory with post-tensioned bars. Each pocket foundation is connected with the adjacent in the longitudinal building direction through full-depth 0.50 m wide beams with strong welded connections. The 6 square columns have a clear height of 7.00 m from the top of the pocket foundation and a side of 0.50 m. The connection with the foundation is cast in laboratory and is considered

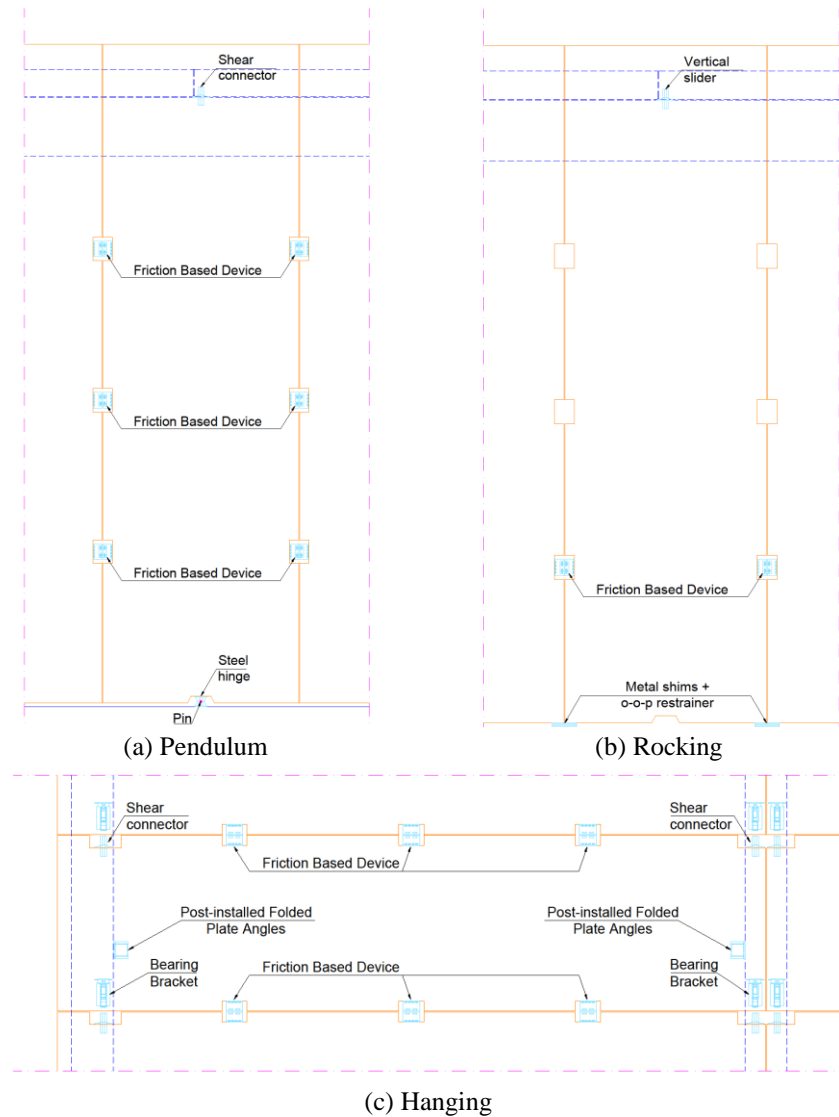


Fig. 2 Cladding panel isostatic arrangements

as a full moment-resisting joint. The 0.50 m wide and 0.75 m deep solid beams are connected with the columns with double-dowel connections. This joint has been considered as a hinged connection for the beam gravity rotations and as a clamped connection for the beam out-of-plane bending, thanks to the horizontal lever arm between the dowels. The slab is made with 7 solid 2.35 m wide, 5.22 m long and 0.35 m deep reinforced concrete panels. It is also connected with double-dowels to the beams. The diaphragm has been further stiffened by 3 floor-to-floor welded rebar connections per interface. The slab members are also provided with large steel plates anchored in the member that have been used to weld the lateral load transmission system that connects the structure with the large ELSA reaction wall through 4 jacks with a capacity of 1000 kN each. In the transverse direction, in correspondence of the 3 column lines, out-of-plane steel bracers are installed for safety matters. They are de-coupled from the structure by a gap of several centimetres, in order to start working only in case of activated collapse, without interfering with the regular tests.

The structure is tested under three configurations:

- Bare frame,
- Vertical panels,
- Horizontal panels.

In the configuration with vertical panels, the frame is provided with 12 solid 2.49×8.40×0.20 m panels, 6 per building longitudinal side (Fig. 1(b)). The panels are provided with a base recess for the accommodation of the hinged base connection and with three recesses along the interfaces with the adjacent panels for the accommodation of the Friction-Based Devices (FBD, Dal Lago *et al.* 2017a). The panels are slightly uncentred with respect to the longitudinal frame direction due to problems of geometric interference with the global connection systems.

In the configuration with horizontal panels, the frame is provided with 16 solid 2.09×8.42×0.20 m panels, 8 per longitudinal side (Fig. 1(c)). The panels are provided with 3 recesses per interface with the adjacent panels for the accommodation of the FBDs.

The structure has been designed according to European structural standards, EN 1991, EN 1992 and EN 1998.

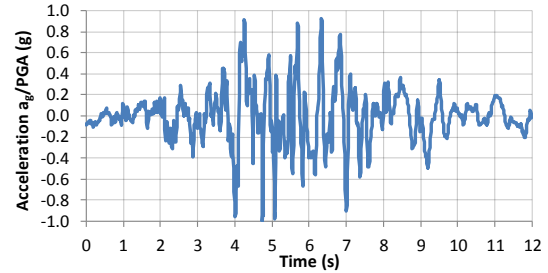
Concrete class C45/55 and reinforcing steel grade B450C were used. The building is placed in a generic high seismicity area in Europe, with a subsoil classified as B. The seismic design was performed through modal analysis with response spectrum, considering a peak ground acceleration for life safety state equal to 0.30 g, which is multiplied by the subsoil amplification factor, equal to 1.2, obtaining 0.36 g. Seismic loading has been considered as acting in one direction only at a time, for compatibility with the mono-axial experimental loading technique. A behaviour factor q equal to 3.00 was adopted. The considered mass, equal to 170 and 175 tons for the specimen with vertical and horizontal cladding panels, respectively, includes half of the mass of the panels.

Three panel structural arrangements are considered in the present paper, namely the pendulum and rocking arrangements for vertical panels and the hanging arrangement for horizontal panels. Specific details about the connections employed are available in Dal Lago (2015).

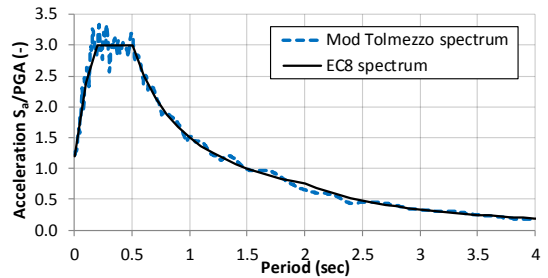
The connections of the pendulum arrangement (Fig. 2(a)) are a central base metallic hinge and a top metallic V-shaped shear connector. When the structure moves, the panels follow it by rotating around the base hinge. One test was carried out after having spread silicone sealant at the panel interfaces from both inner and outer sides. Several tests were carried out with the installation of dissipative FBD connections in the vertical recesses of the panels.

The connections of the rocking arrangement (Fig. 2(b)) are a simple base support on metallic shims with an out-of-plane angle restrainer and a top metallic V-shaped shear connector employed as a vertical slider. When the structure moves, the panels follow it by rotating around their base corners while lifting up. Several tests were carried out with the installation of a single dissipative FBD connection per interface in the bottom vertical recesses of the panels.

The connections of the hanging arrangement (Fig. 2(c))



(a) Acceleration time history



(b) response spectrum

Fig. 3 Modified Tolmezzo accelerogram

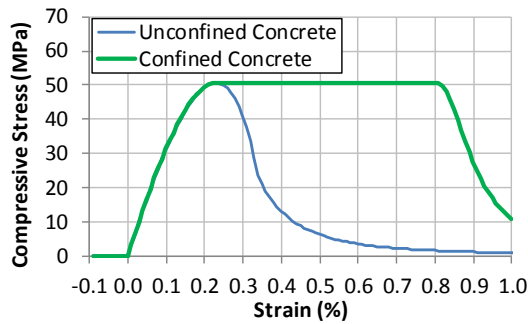
are two horizontally sliding metallic bracket base supports and two top metallic V-shaped shear connectors. When the structure moves, the panels follow it by displacing over the base brackets. Several tests were carried out with the installation of dissipative FBD connections or W-shaped Folded Plate Angles (FPAs, Dal Lago *et al.* 2018b).

The seismic tests were carried out using the pseudo-dynamic technique (Molina *et al.* 2013) through the application of the Modified Tolmezzo accelerogram (Fig. 3) scaled at different levels of PGA. The original signal, recorded during the Friuli earthquake of 1976 in North-East Italy, was artificially enriched in frequencies to make its

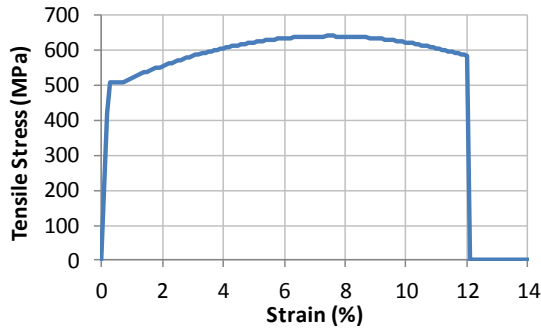
Table 1 List of considered test configurations

Test ID	Prototype	Arrangement	Conn./Joints	System	PGA
#1	bare frame	n/a	n/a	n/a	0.10g
#2	bare frame	n/a	n/a	n/a	0.36g
#3	vertical panels	pendulum	none	isostatic	0.10g
#4	vertical panels	pendulum	silicone	isostatic	0.10g
#5	vertical panels	pendulum	1FBD/75 kN	dissipative	0.36g
#6	vertical panels	pendulum	2FBD/75 kN	dissipative	0.36g
#7	vertical panels	pendulum	2FBD/75 kN	dissipative	0.72g
#8	vertical panels	pendulum	3FBD/75 kN	dissipative	0.18g
#9	vertical panels	pendulum	3FBD/75 kN	dissipative	0.36g
#10	vertical panels	pendulum	3FBD/75 kN	dissipative	0.72g
#11	vertical panels	pendulum	3FBD/75 kN	dissipative	1.00g
#12	vertical panels	rocking	none	isostatic	0.18g
#13	vertical panels	rocking	none	isostatic	0.18g
#14	vertical panels	rocking	1FBD/50 kN	dissipative	0.36g
#15	horizontal panels	hanging	1FBD/75 kN	dissipative	0.36g
#16	horizontal panels	hanging	2FBD/75 kN	dissipative	0.36g
#17	horizontal panels	hanging	2FBD/75 kN	dissipative	0.54g
#18	horizontal panels	hanging	2FPA	dissipative	0.18g
#19	horizontal panels	hanging	2FPA	dissipative	0.36g

PSD: Pseudo-dynamic; FBD: Friction Based Device; FPA: Folded Plate Angle (W shape)



(a) Concrete stress vs strain diagram



(b) Steel stress vs strain diagram

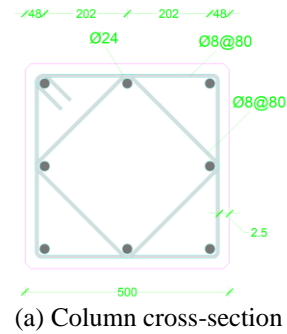
Fig. 4 Stress-strain relationships for (a) concrete and (b) reinforcing steel

spectrum compatible with the one given by EN 1998. A mass of 175 tons was also considered for the bare frame structure, in order to have a direct comparison with the results from the tests on the cladded structure. The complete list of the 19 seismic tests analysed in this paper is given in Table 1.

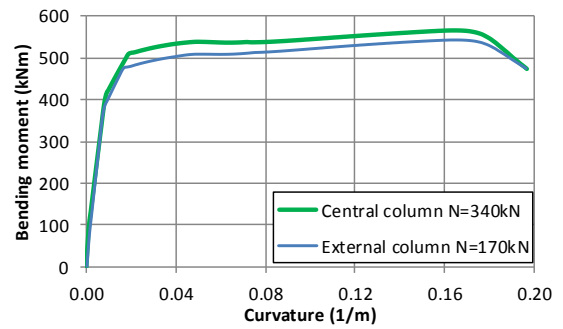
3. Numerical models

Four finite element models, one for the bare frame and one per each panel arrangement, were developed with the computer program Straus7 (G+D Computing 2010) with the aim to predict the experimental results prior to the execution of the tests, to check for displacements and forces to be compatible with the setup and the test programme. This software contains all numerical tools needed to tackle the problem, whilst keeping a mixed user audience between academicians and practitioners.

The frame was modelled in the same way for all the considered structural configurations. Each $7 \times 0.5 \times 0.5$ m column is modelled with 28 beam elements. All columns are clamped at the base and linked to the beams with master/slave links coupling all degrees of freedom. The columns were modelled with distributed plasticity through the attribution of non-linear moment curvature diagrams obtained from equilibrium based on the mean mechanical properties of concrete and reinforcing steel. A Sargin (Sargin and Handa 1969) model was used for unconfined concrete, while a modified version with constant peak load up to the ultimate strain as defined in the Model Code 10 (fib 2010) was used to account for the core confinement provided by the transversal reinforcement (Fig. 4(a)). The



(a) Column cross-section



(b) Non-linear moment vs curvature diagrams

Fig. 5 Non-linear model of the columns: (a) cross-section of the column and (b) corresponding non-linear moment-curvature diagrams

tensile resistance of concrete was neglected. This assumption is justified by the scope of the numerical model, which is to simulate the seismic performance of a structure which already attained cracking (from pre-tests) at the beginning of all tests. An elastic-yielding-parabolic model has been used for steel (Fig. 4(b)). Based on the different axial loads of the central and external columns, both equally reinforced with 8 $\phi 24$ longitudinal bars confined by $\phi 8 @ 80$ mm stirrups placed as per Fig. 5(c), the two corresponding non-linear moment versus curvature diagrams are shown in Fig. 5(d). The stirrup spacing was kept constant through the height of the column due to the high concentrated shear forces occurring along the height in the configuration with horizontal cladding panels and FBDs.

The program automatically assigns the pertinent length of plasticisation at each analysis step based on the integration at Gauss-Lobatto points distributed along the elements. A Takeda hysteretic model was assigned to the elements (Takeda *et al.* 1970). This hysteretic model, as well as the other models employed, does not account for cyclic deterioration.

Each $8.0 \times 0.8 \times 0.4$ m solid beam is divided into several elastic beam elements, in order to accommodate the positions of the connections with the cladding panels. The end rotation around the orthogonal horizontal axis is left free, simulating a perfectly hinged vertical connection over the column. Each $5.0 \times 2.5 \times 0.35$ m solid slab element is modelled with elastic beam elements. Their ends are connected with the beams through master/slave links coupling all degrees of freedom. The rotation around the orthogonal horizontal axis is left free, simulating a perfectly hinged vertical connection over the beam.

The mass is lumped in the slab members only, dividing

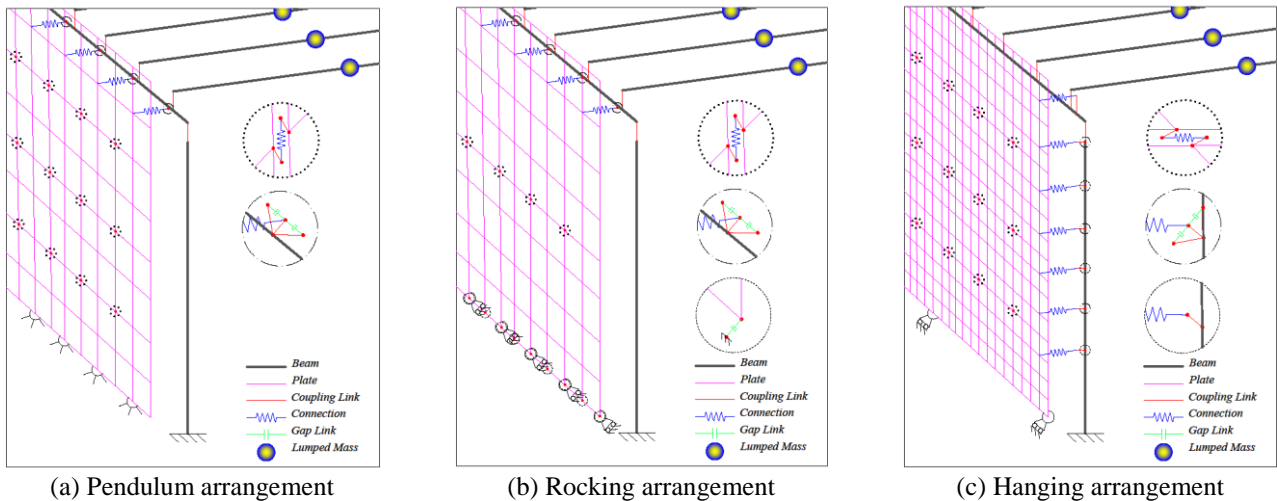


Fig. 6 Finite element models

the global mass by their number. This procedure, while differing from the real mass distribution, is necessary to simulate the results of the pseudo-dynamic tests, where the mass was considered lumped at the roof level.

Fig. 6 shows a schematic picture of the models with reference to each panel configuration.

The $8.4 \times 2.5 \times 0.16$ m vertical and $7.0 \times 2.1 \times 0.16$ m horizontal solid cladding panels were modelled with rectangular elastic plate/shell elements, with regular sides. The different mesh is due to the need of having a node in the different position of the connections with the structure. Vertical panels with pendulum arrangement (Fig. 6(a)) were connected with a central hinge at the bottom to the ground and with a central connection element with the beam. This connection element was provided with a high horizontal stiffness both in the plane and out of the plane of the panels, while its vertical displacement was released. Due to the need of simulating the presence of 3.0 mm of clearance of the top shear connector, the connection element was coupled with horizontal gap elements acting in compression only after the gap closing, imposed equal to 1.5 mm for each gap element. The eccentricity of the external nodes of the gap elements with the beam was covered by coupling links.

Vertical panels with rocking arrangement (Fig. 6(b)) were modelled with horizontal displacement base restraints and vertical contact elements for all the nodes at the base of the panels and a top element arrangement similar to the one previously described for the pendulum system. Horizontal panels with hanging arrangement (Fig. 6(c)) were modelled with the above-described procedure for the shear connectors, while the rigid support brackets were modelled with links coupling vertical and out-of-plane displacements, while leaving the panel free to slide horizontally. The base panels were similarly restrained to the ground.

The dissipative connections used in the simulations were modelled with lumped plasticity through connection elements to which non-linear load-displacement diagrams (Fig. 7) were attributed in their axial direction. These connection elements were then linked to the nodes of the panels and of the structure through links coupling all

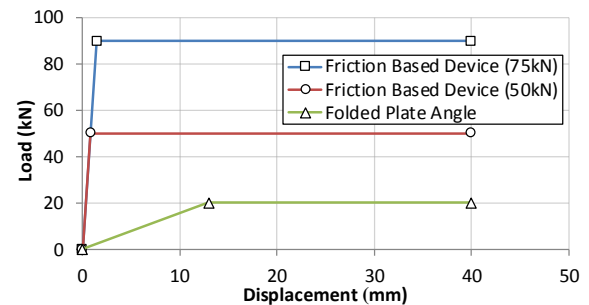


Fig. 7 Non-linear models of the dissipative connections

displacements except the one along the axis of the element. Simplified macro-models were calibrated on the basis of the experimental characterization obtained through local tests on the single devices. FBDs were modelled with an elastic-plateau relationship with initial stiffness of 60 kN/mm, where the plateau load corresponded to the friction activation thresholds. Due to the moderate uncertainty related to the definition of the activation threshold, depending on several parameters (Dal Lago *et al.* 2017a), the threshold of the device designed to slide at 75 kN was calibrated after the preliminary tests performed on the full-scale structural assemblies, where a higher mean load equal to 90 kN was observed. The device designed to slide at 50 kN showed compatible results under testing and therefore its model did not need to be refined. FPAs (Dal Lago *et al.* 2018b) were modelled with a similar technique, with the elastic stiffness much lower with respect to FBDs (1.50 kN/mm).

A kinematic hardening cyclic model has been assigned for both connection devices.

Silicone sealant was considered perfectly elastic with a tangential modulus G of 0.25 MPa, as calibrated from experimental tests (Dal Lago *et al.* 2017b). Due to its remarkable flexibility with respect to the concrete panels, the contribution of silicone was lumped in the central spring by multiplying the sectional stiffness of the silicone strips by their total area at the panel interface.

All analyses were carried out imposing a Rayleigh viscous damping of 2% to a wide range of periods, from

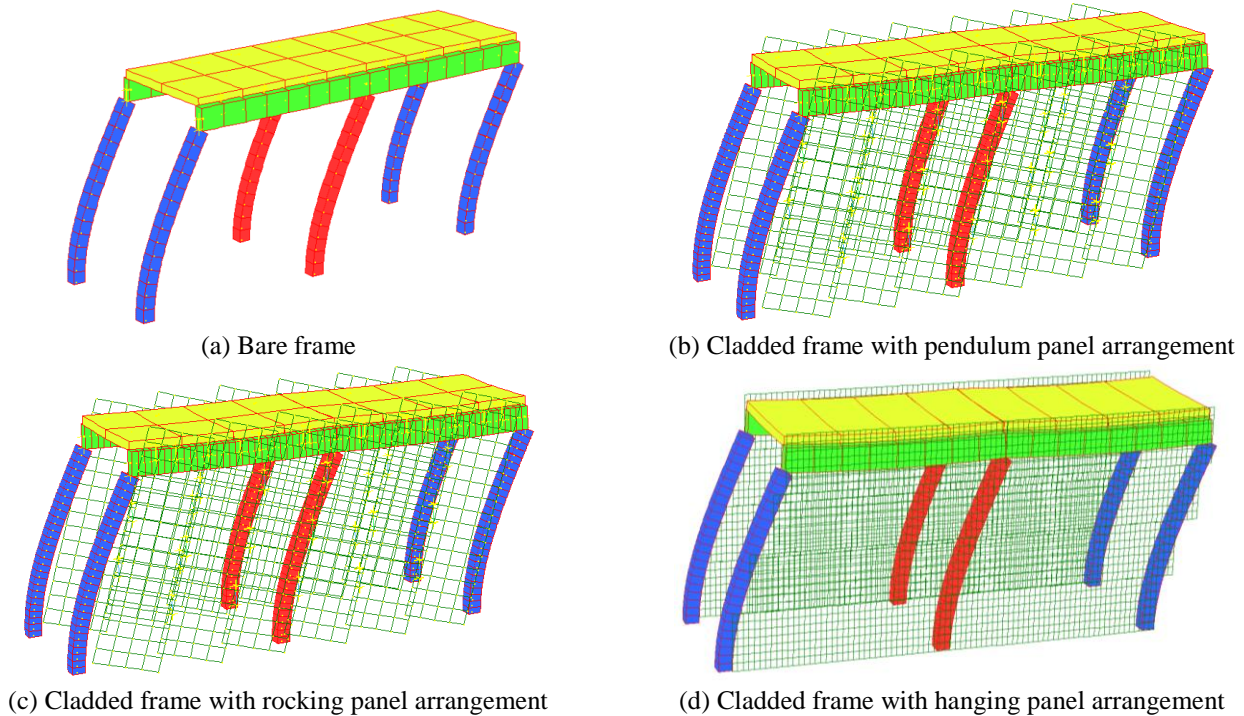


Fig. 8 Deformed structural shape

1.35 s associated to the natural vibration mode of the bare frame considering a halved column stiffness as suggested by EuroCode 8 (EN 1998-1) to account for cracking to the 0.20 s associated to the natural vibration mode of the structure provided with dissipative connections acting in elastic range. This wide range of periods was chosen so to use the same model for all the structural configurations without the risk of over-damping the analyses or not being able to directly compare them. As a matter of fact, all intermediate values between 0.20 and 1.35 s will be damped for effective values lower than 2%. The value of viscous damping was kept at this low value to better simulate the results of the pseudo-dynamic tests, where no explicit viscous damping was introduced, while avoiding problems of numerical instability.

All dynamic non-linear analyses have been carried out including *P*-Delta second order effects. The numerical models can predict a global collapse due to second order effect, while each possible local failure should be identified during post-processing by checking that the deformation/load of the specific connection or component does not overcome the limit values.

Fig. 8 shows the deformed shape of the models that were developed.

4. Numerical simulation of seismic pseudo-dynamic tests and comparison with experimental results

4.1 Bare frame structure

The bare frame structure exhibited a flexible seismic behaviour, characterised by large displacements with relatively low base shear forces. The simulation of the test

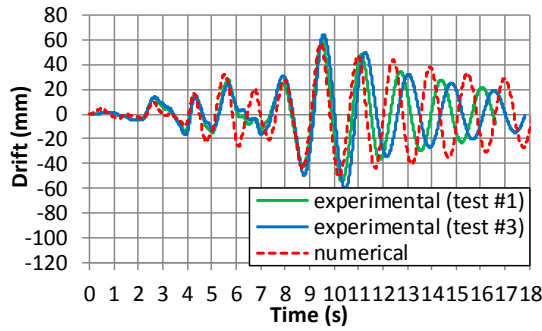
with $PGA=0.10$ g (Figs. 9(a), (b)) shows that the elastic initial branch with plain cross-sectional stiffness, induced by the dead compressive loads, is not caught by the test results, showing an elastic stiffness which equals the cracked stiffness of the numerical model. The difference is however limited, and the trend was correctly simulated, with a difference occurred in the free-vibration motion at the end of the test, with the simulated structure vibrating slightly more flexibly.

In the test with $PGA=0.36$ g, the experimental trend is again correctly caught by the numerical simulation, with a vibrational scatter in the post-earthquake quasi-free-vibration field (Figs. 9(c), (d)). This suggests that the actual value of viscous damping in the elastic field (these vibrations occurred in a displacement amplitude field lower than the yielding one) is higher with respect to the conservative assumption previously described.

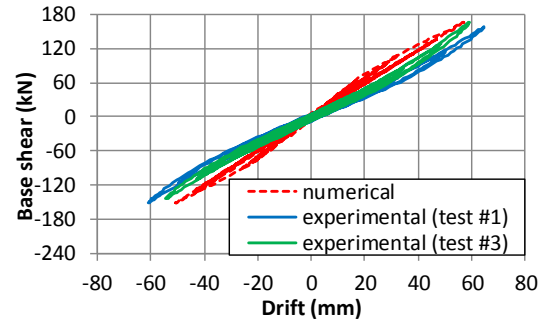
The tested structure was damaged only in the pseudo-dynamic test with $PGA=0.36$ g. In this test, which has been the last performed in the test sequence, the base of the columns attained cracking and yielding, as also found out from the numerical simulation. In all other tests, the whole structure was fully undamaged, with the exception of cracking along the height of the column, which however did not bring to yielding of the reinforcement, with the developed cracks closing after each test.

4.2 Structure cladded by vertical panels with pendulum arrangement

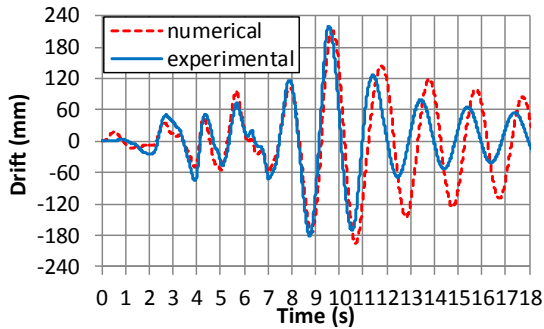
The installation of vertical cladding panels connected with a pendulum arrangement does not provide any relevant change in the seismic response, as it can be observed from the comparison of the two experimental curves in Figs. 9(a),



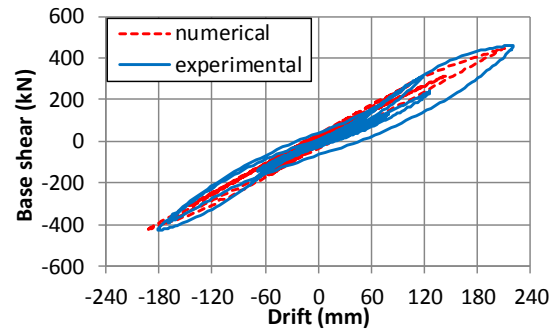
(a) 0.10 g – Drift time history



(b) 0.10 g – Base shear vs Drift

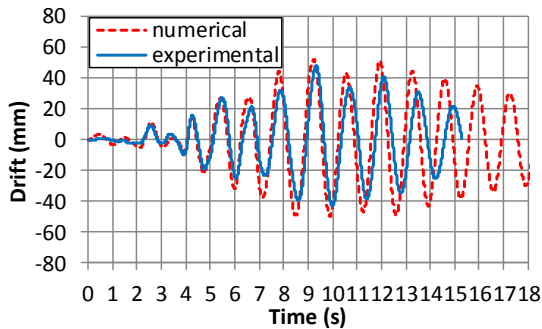


(c) Bare frame – 0.36 g – Drift time history (test #2)

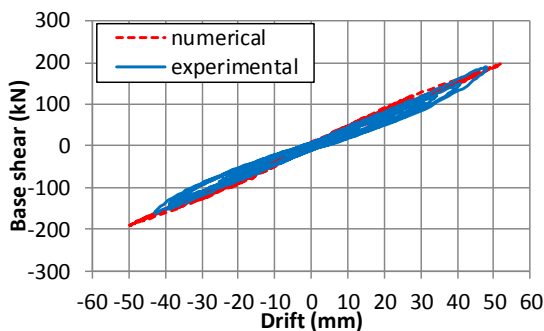


(d) Bare frame – 0.36 g – Base shear vs Drift (test #2)

Fig. 9 Tests on the bare frame and on the cladded frame with vertical pendulum arrangement



(a) 0.10 g – Drift time history



(b) 0.10 g – Base shear vs Drift

Fig. 10 Tests on the cladded frame with vertical pendulum panels and silicone (test #4)

(b), and the numerical model provides identical results if the panels are considered or not. It has to be noted that this is true for the considered tests, where the seismic mass has been kept at the same value in the pseudo-dynamic test procedure for the two structures, having as objective a comparison of the two behaviours, while in reality the

installation of the panels would add a relevant seismic mass to that of the bare frame.

The comparison with the test results on the building having interposed silicone sealant in between the pendulum panels shows a good prediction by the numerical model (Fig. 10), which confirms the validity of the silicone stiffness as described above. The quasi-free-vibration trend shows some differences, due to the conservative value of viscous damping employed, which neglects on the safe side the small hysteresis occurring within the silicone strips. When FBDs are installed at the panel interfaces, the behaviour relevantly modifies, turning into highly non-linear. The non-linearity is due to the activation of the devices when their load overcomes the friction threshold, which occurs at low vertical relative displacement between the panels, due to the high pre-activation elastic stiffness of the devices.

All the results related to the tests performed on the pendulum panel configuration with FBDs are shown in Fig. 11 in comparison with the numerical prediction. The single analysis with 3 FBDs per interface and PGA of 1.00 g stopped at about 8.5 mm because of numerical divergence, however providing a satisfactory response up to that point. Despite the high non-linearity involved, the model satisfactorily simulates the seismic response in all cases. It can be observed especially from the tests with many FBDs and low PGA that the hysteresis is strongly influenced by the pinching effect occurring within few millimetres from zero, attributable to the allowance of the panel-to-beam devices. If considering the test with 3 FBDs and PGA of 0.18 g (Figs. 11(g), (h)), the response is practically elastic (no activation of the FBDs), and the vibration occurs around the allowance of the panel-to-beam devices. The numerical model is able to catch this behaviour thanks to the use of the

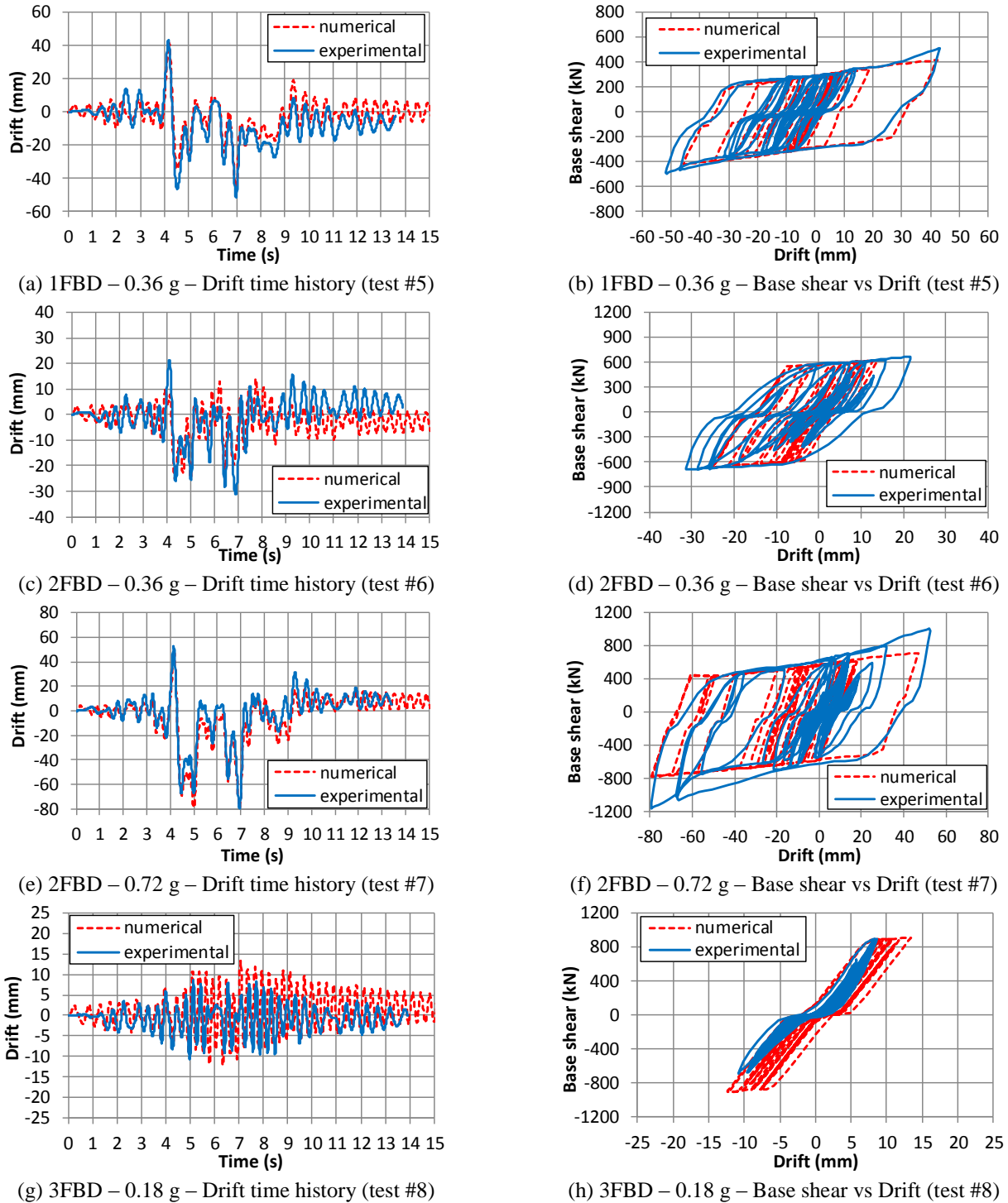


Fig. 11 Tests on the cladded frame with vertical pendulum panels and FBDs

gap element connections in the position of the panel-to-beam devices. The importance of considering the gap in the analyses decreases with increasing PGA, since the influence of its fixed value (around 3 mm) becomes small if compared to high structural drifts.

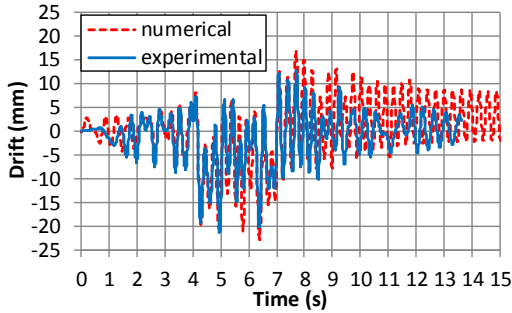
It can be noted from the base shear versus drift diagrams that a variable hardening branch was not caught by the models (Fig. 11(b), (f), (k), (m)).

This effect is due to the unavoidable uncertainties embedded into the frictional hysteresis of the FBDs, as

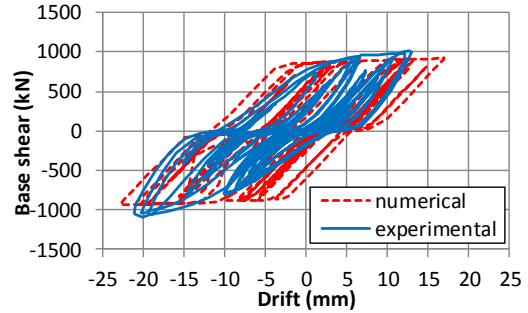
identified by Dal Lago *et al.* (2017a), and is deemed to randomly occur. As such, this effect could not be caught by the elastic-plateau model employed for each single device (Fig. 7).

4.3 Structure cladded by vertical panels with rocking arrangement

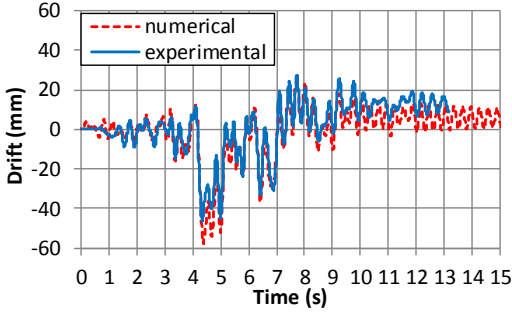
When the vertical panels are connected with a rocking arrangement, the hysteresis changes completely. An initial



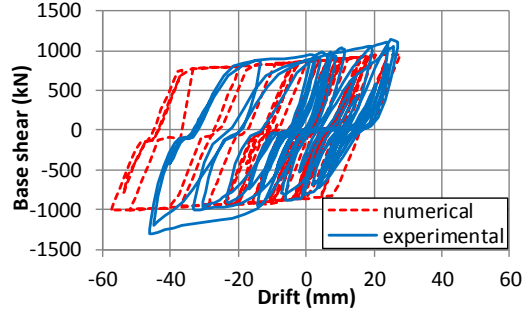
(h) 3FBD – 0.36 g – Drift time history (test #9)



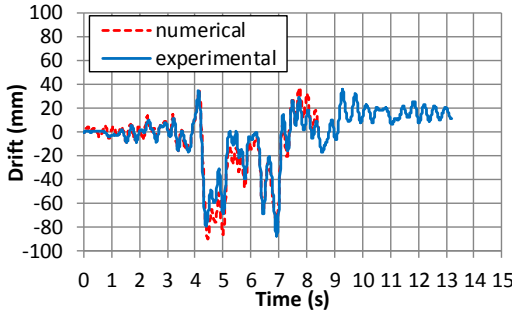
(i) 3FBD – 0.36 g – Base shear vs Drift (test #9)



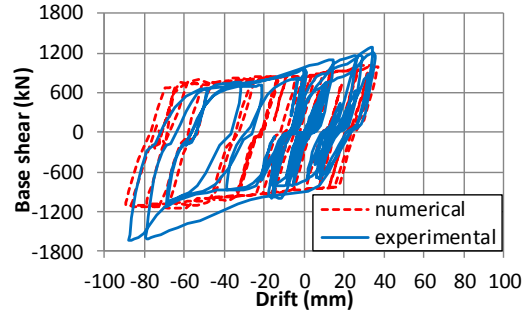
(j) 3FBD – 0.72 g – Drift time history (test #10)



(k) 3FBD – 0.72 g – Base shear vs Drift (test #10)

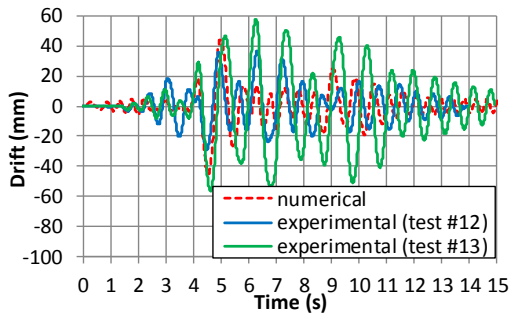


(l) 3FBD – 1.00 g – Drift time history (test #11)

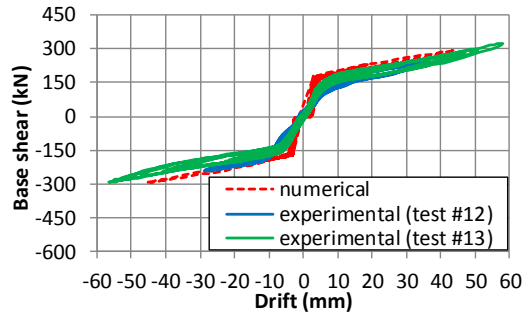


(m) 3FBD – 1.00 g – Base shear vs Drift (test #11)

Fig. 11 Continued



(a) 0.18 g – Drift time history



(b) 0.18 g – Base shear vs Drift

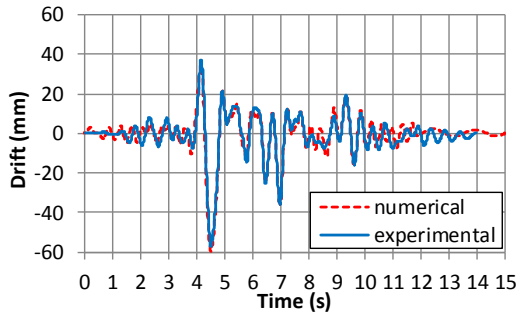
Fig. 12 Tests on the cladded frame with vertical rocking panels

stiff branch displays up to uplift of the panels around a corner, which occurs when the stabilising bending moment due to their own weight is overcome by the one produced by the horizontal load. After this point, the stiffness comes back to the one of the bare frame.

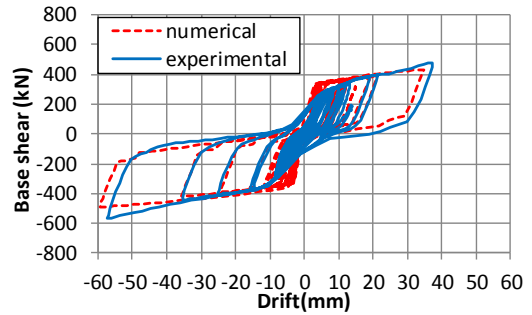
When unloading, the plot follows the loading branch, providing this highly non-linear behaviour with null dissipation of energy, at least prior to yielding of the column bases.

Two tests were carried out on this panel connection arrangement, whose results are shown in Fig. 12. The first test was repeated after evidence of a non-standard behaviour of the panel-to-beam connections, which become vertical sliders in this configuration.

The experimental results from the two formally equal tests show relevant discrepancies, confirming that the sliding mechanism of the connection is characterised by a non-repeatable response. However, their hysteretic shape is

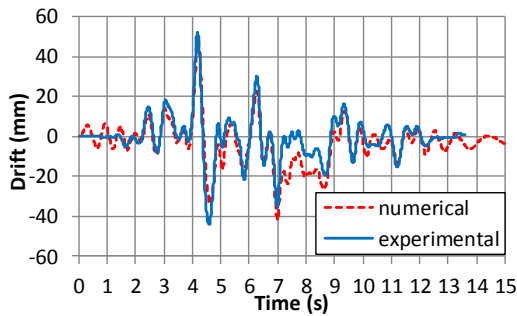


(a) 1FBD – 0.36 g – Drift time history

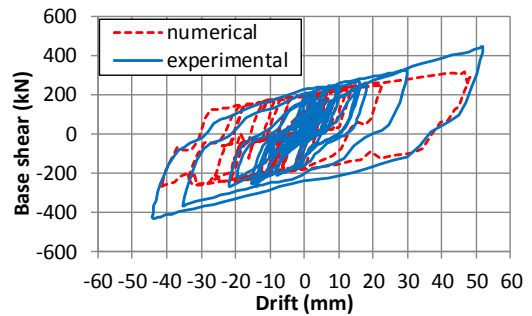


(b) 1FBD – 0.36 g – Base shear vs Drift

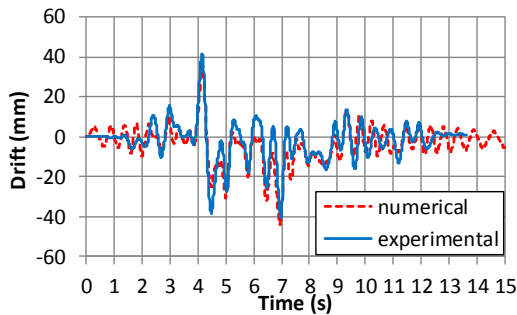
Fig. 13 Tests on the cladded frame with vertical rocking panels and FBDs (test #14)



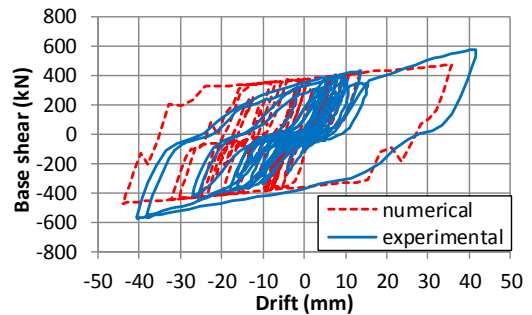
(a) 1FBD – 0.36 g – Drift time history (test #15)



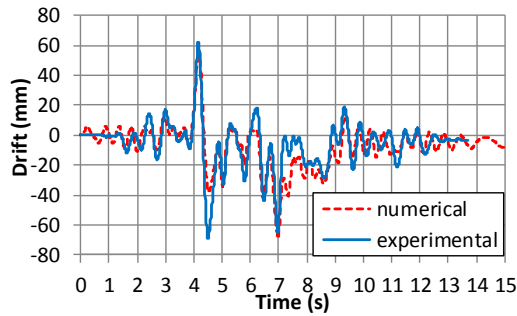
(b) 1FBD – 0.36 g – Base shear vs Drift (test #15)



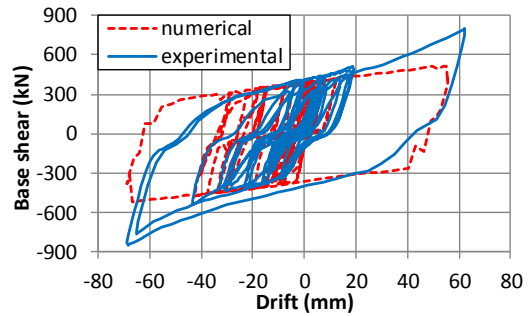
(c) 2FBD – 0.36 g – Drift time history (test #16)



(d) 2FBD – 0.36 g – Base shear vs Drift (test #16)



(e) 2FBD – 0.54 g – Drift time history (test #17)



(f) 2FBD – 0.54 g – Base shear vs Drift (test #17)

Fig. 14 Tests on the cladded frame with horizontal hanging panels and FBDs

the same (Fig. 12(b)). The numerical simulation provides a drift time history curve which falls in between the ones resulting from the two tests.

Also in this case, the introduction of a gap element in the panel-to-beam joint allows to account for a non-instantaneous uplift of the panels consequent to structural displacement. It must be noted that the experimental curves are much softer in the initial branch. This occurs since the panel-to-beam connections are installed with a random

position with respect to their allowances, while the numerical model reflects the situation in which all connections are installed perfectly in the middle of their allowance, leading to a sudden stiff increase of load when all connections touch the end of the gap.

When FBDs are installed in the panel interfaces, the hysteresis turns into flag-shaped (Fig. 13), adding to the elastic restoring action of the panels a relevant energy dissipation capacity. The analysis of this configuration

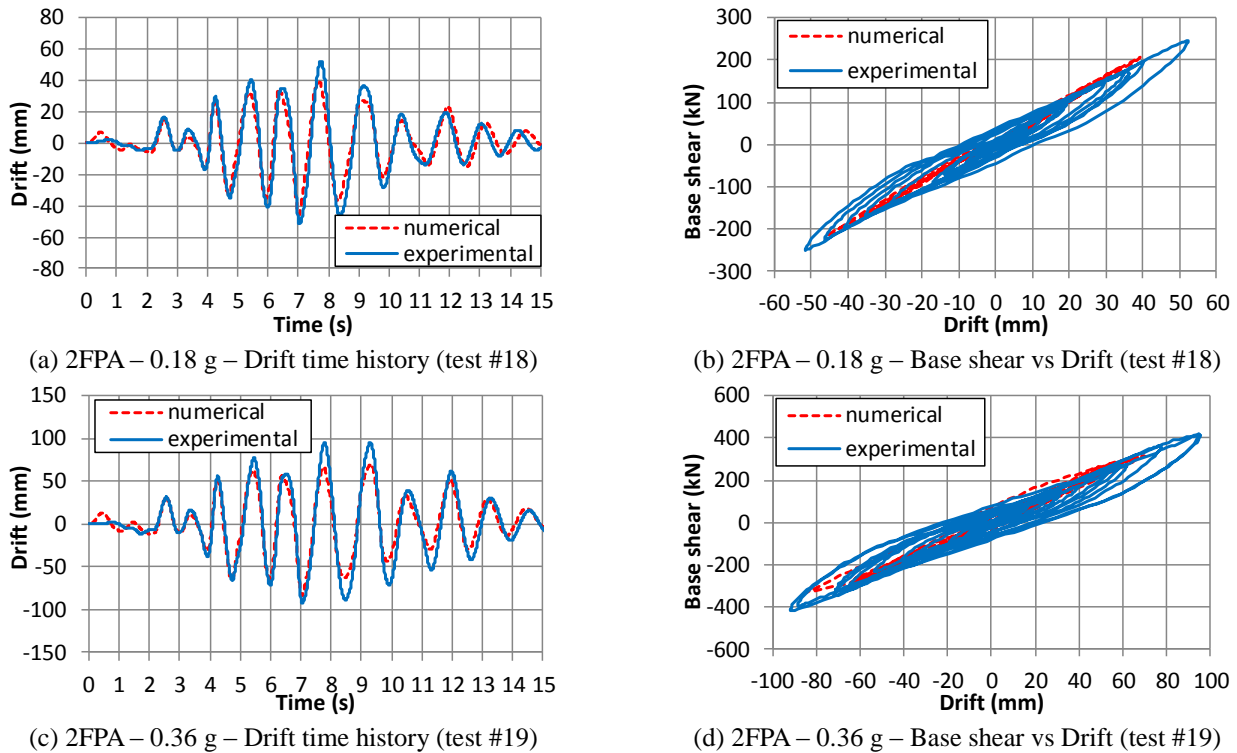


Fig. 15 Tests on the cladded frame with horizontal hanging panels and FPAs

provides a very good estimation of the seismic response of the assembly, which suggests that the introduction of FBDs regulates the hysteretic behaviour of the panel-to-beam connections.

4.4 Structure cladded by horizontal panels with hanging arrangement

The results of the tests carried out on the structure with horizontal hanging panels connected with panel-to-panel mutual FBD connections are shown in Fig. 14.

All numerical simulations provide a good correspondence of the drift time history, showing the ability to capture also the peculiar phenomenon of the intermediate indentations in the base shear versus drift curves, due to the instantaneous counter-acting displacements of different rows of FBDs, which is more evident in the numerical curves.

In all these tests, the hysteretic curves show a tendency to the rise of the load at larger displacements which is not caught by the numerical model. In addition to the previously discussed issue of the non-plateau behaviour of the FBDs, also friction occurring at the bracket connection might have summed its contribution.

The results of the tests with FPAs are shown in Fig. 15. The numerical curve is pseudo-linear up to yielding of the column bases, while the numerical curve shows some dissipation of energy, which occurred by friction at the panel-to-column bracket connections. Nevertheless, the drift time history is predicted with accuracy, even if a displacement scatter is observed in correspondence of the stronger peaks.

5. Conclusions

A numerical simulation procedure for predicting the seismic response of precast structures with cladding panels was proposed for various connection arrangements of the panels. The procedure was consistently applied to a precast frame structure prototype tested within the framework of the Safeccladding research project. Based on the comparison of the numerical results with the experimental ones, the following conclusions can be drawn:

- The analyses provided a sound prediction of the whole experimental programme, comprising tests on both bare and cladded structure;
- The higher initial stiffness of the structure predicted by the frame model due to the plain stiffness of the cross-section induced by the axial load is not observed in the experimental results, displacing according to the cracked stiffness since small displacements; however, the axial stress on the precast columns of the specimen, as typical for the columns of precast industrial buildings, is low and the response is not relevantly affected by this phenomenon;
- The comparison of the quasi-free-vibration motion of the bare frame tests shows that the assumed viscous damping, Rayleigh type with 2% at remarkably distant frequencies, is too conservative for strong ground motions;
- The effect of the allowances of the panel-to-structure connections modifies the response when the panels provide a restoring or dissipative action. This issue, which needs a more sophisticated modelling with gap elements, can be neglected for vertical pendulum and

horizontal hanging panel arrangements, unless dissipative mutual connections are installed in between the panels;

- The effect of the standard allowances of few millimetres highly affects the seismic response for isostatic rocking or dissipative systems when the displacements are limited, typically for weak earthquakes. The high displacement related to the occurrence of strong earthquakes reduces the effect of the allowances. To this aim, the effect of the allowances could be neglected in the model when the expected structural displacement is at least 10 times its value;
- The elastic shell modelling of the panels provided a good correspondence with the experimental results. However, in all the analysed cases the panels practically acted as rigid bodies without any cracking or damage, which suggests that simplified modelling could be employed for a lighter model, even though the use of rigid links may jeopardise the numerical stability of the solver;
- The elastic-plateau mechanical model of Friction-Based Devices (FBDs) provided results in general accordance with the experimental evidence. However, the FBDs showed tendencies to harden after activation. This hardening branch, observed also in the local tests on single devices, is however characterised by a certain degree of randomness. As such, the proposed model is suggested to safely predict the mechanical behaviour of the devices;
- Hanging panels have an additional source of dissipation consisting in the friction occurring at the bearing bracket panel-to-column sliding device, which is also quite random, and which does not relevantly affect the structural response. As such, it is suggested to neglect this contribution into the model;
- As a clear outcome of the work described in the paper, the influence of the cladding panel connection systems on the seismic response of precast frame structures can be of fundamental importance. The proposed techniques are suggested to be employed in the sophisticated structural modelling of precast frame buildings with various arrangements of cladding panels, to be studied through non-linear analysis. The effectiveness of simplified assumptions, necessary to perform more traditional linear analysis fully accounting for the panel-frame interaction, shall be investigated and validated in the near future, even though equivalent elastic design will lose accuracy the more the coupled structural system is influenced by non-linear mechanical and geometrical effects.

Acknowledgments

The research described in this paper was financially supported by the Safecladding project (Grant Agreement No. 314122/2012) funded by the European Commission within the 7th framework programme, coordinated by Mr. Alessio Rimoldi of BIBM under the technical supervision of Prof. Giandomenico Toniolo from Politecnico di Milano.

The tests simulated in the paper were carried out at the ELSA laboratory of the Joint Research Centre of the European Commission in Ispra, Italy, by the team headed by Dr. Paolo Negro.

References

- Babić, A. and Dolšek, M. (2016), "Seismic fragility functions of industrial precast building classes", *Eng. Struct.*, **118**, 357-370.
- Baird, A., Palermo, A. and Pampanin, S. (2012), "Experimental and numerical validation of seismic interaction between cladding systems and moment resisting frames", *Proceedings of the 15th World Conference on Earthquake Engineering*, Lisbon, Portugal, September; Paper No. 1981.
- Batalha, N., Rodrigues, H. and Varum, H. (2019), "Seismic performance of RC precast industrial buildings-learning with the past earthquakes", *Innov. Infrastr. Sol.*, **4**(1), 4.
- Belleri, A. (2017), "Displacement based design for precast concrete frames with not-emulative connections", *Eng. Struct.*, **141**, 228-240.
- Belleri, A., Brunesi, E., Nascimbene, R., Pagani, M. and Riva, P. (2015), "Seismic performance of precast industrial facilities following major earthquakes in the Italian territory", *J. Perform. Constr. Facil.*, **29**(5), 04014135.
- Belleri, A., Cornali, F., Passoni, C., Marini, A. and Riva, P. (2018), "Evaluation of out-of-plane seismic performance of column-to-column precast concrete cladding panels in one-storey industrial buildings", *Earthq. Eng. Struct. Dyn.*, **47**(2), 397-417.
- Belleri, A., Schoettler, M.J., Restrepo, J. and Fleishman, R.B. (2014), "Dynamic behavior of rocking and hybrid cantilever walls in a precast concrete building", *ACI Struct. J.*, **111**(3), 661-672.
- Belleri, A., Torquati, M., Marini, A. and Riva, P. (2016), "Horizontal cladding panels: in-plane seismic performance in precast concrete buildings", *Bull. Earthq. Eng.*, **14**(4), 1103-1129.
- Biondini, F. and Toniolo, G. (2009), "Probabilistic calibration and experimental validation of the seismic design criteria for one-storey concrete frames", *J. Earthq. Eng.*, **13**, 426-462.
- Biondini, F., Dal Lago, B. and Toniolo, G. (2013), "Role of wall panel connections on the seismic performance of precast structures", *Bull. Earthq. Eng.*, **11**(4), 1061-1081.
- Bournas, D., Negro, P. and Taucer, F. (2013b), "Performance of industrial buildings during the Emilia earthquakes in Northern Italy and recommendations for their strengthening", *Bull. Earthq. Eng.*, **12**(5), 2383-2404.
- Bournas, D.A., Negro, P. and Molina, F.J. (2013a), "Pseudodynamic Tests on a full-scale 3-storey precast concrete building: behaviour of the mechanical connections and floor diaphragms", *Eng. Struct.*, **57**, 609-627.
- Brunesi, E., Nascimbene, R., Bolognini, D. and Bellotti, D. (2015a), "Experimental investigation of the cyclic response of reinforced precast concrete frames structures", *PCI J.*, **2**, 57-79.
- Brunesi, E., Nascimbene, R., Deyanova, M., Pagani, C. and Zambelli, S. (2015b), "Numerical simulation of hollow steel profiles for lightweight concrete sandwich panels", *Comput. Concrete*, **15**(6), 951-972.
- Buratti, N., Minghini, F., Ongaretto, E., Savoia, M. and Tullini, N. (2017), "Empirical seismic fragility for the precast RC industrial buildings damaged by the 2012 Emilia (Italy) earthquakes", *Earthq. Eng. Struct. Dyn.*, **46**(14), 2317-2335.
- Cohen, J.M. and Powell, G.H. (1993). "A design study of an energy dissipating cladding system", *Earthq. Eng. Struct. Dyn.*, **22**(7), 617-632.
- Dal Lago, B. (2015), "Seismic performance of precast structures

- with dissipative cladding panel connections”, Ph.D. Dissertation, Politecnico di Milano, Italy.
- Dal Lago, B. and Ferrara, L. (2018), “Efficacy of roof-to-beam mechanical connections on the diaphragm behaviour of precast decks with spaced roof elements”, *Eng. Struct.*, **176**, 681-696.
- Dal Lago, B. and Lamperti Tornaghi, M. (2018), “Sliding channel cladding connections for precast structures subjected to earthquake action”, *Bull. Earthq. Eng.*, **16**(11), 5621-5646.
- Dal Lago, B. and Molina, F.J. (2018), “Assessment of a capacity spectrum design approach against cyclic and seismic experiments on full-scale precast RC structures”, *Earthq. Eng. Struct. Dyn.*, **47**(7), 1591-1609.
- Dal Lago, B., Bianchi, S. and Biondini, F. (2018a), “Diaphragm effectiveness of precast concrete structures with cladding panels under seismic action”, *Bull. Earthq. Eng.*, **17**(1), 473-495.
- Dal Lago, B., Biondini, F. and Toniolo, G. (2017a), “Friction-based dissipative devices for precast concrete panels”, *Eng. Struct.*, **147**, 356-371.
- Dal Lago, B., Biondini, F. and Toniolo, G. (2018b), “Experimental investigation on steel W-shaped folded plate dissipative connectors for precast cladding panels”, *J. Earthq. Eng.*, **22**(5), 778-800.
- Dal Lago, B., Biondini, F. and Toniolo, G. (2018c), “Experimental tests on multiple-slit devices for precast concrete panels”, *Eng. Struct.*, **167**, 420-430.
- Dal Lago, B., Biondini, F. and Toniolo, G. (2018d), “Seismic performance of precast concrete structures with energy dissipating cladding panel connection systems”, *Struct. Concrete*, **19**, 1908-1926.
- Dal Lago, B., Biondini, F., Toniolo, G. and Lamperti Tornaghi, M. (2017b), “Experimental investigation on the influence of silicone sealant on the seismic behaviour of precast façades”, *Bull. Earthq. Eng.*, **15**(4), 1771-1787.
- Dal Lago, B., Negro, P. and Dal Lago, A. (2018e), “Seismic design and performance of dry-assembled precast structures with adaptable joints”, *Soil Dyn. Earthq. Eng.*, **106**, 182-195.
- Dal Lago, B., Toniolo, G. and Lamperti Tornaghi, M. (2016), “Influence of different mechanical column-foundation connection devices on the seismic behaviour of precast structures”, *Bull. Earthq. Eng.*, **14**(12), 3485-3508.
- EN 1991-1:2004 (2004), Eurocode 1: Actions on Structures. Part 1: General Actions, European Committee for Standardization, Brussels, Belgium.
- EN 1992-1-1:2005 (2005), Eurocode 2: Design of Concrete Structures. Part 1-1: General Rules and Rules for Buildings, European Committee for Standardization, Brussels, Belgium.
- EN 1998-1:2004 (2004), Eurocode 8: Design of Structures for Earthquake Resistance. Part 1: General Rules, Seismic Actions and Rules for Buildings, European Committee for Standardization, Brussels, Belgium.
- fib (2010), Model Code for Concrete Structures, Fédération Internationale du Béton/International Federation for Structural Concrete, Lausanne, Switzerland.
- Fischinger, M., Kramar, M. and Isaković, T. (2008), “Cyclic response of slender RC columns typical of precast industrial buildings”, *Bull. Earthq. Eng.*, **6**(3), 519-534.
- Fleischman, R.B., Sause, R., Pessiki, S. and Rhodes, A.B. (1998), “Seismic behavior of precast parking structure diaphragms”, *PCI J.*, **43**(1), 38-53.
- G+D Computing (2010), *Using Strand7 (Straus7) - Introduction to the Strand7 finite element analysis system*, Ed. 3, Strand7 Pty Limited, Sidney, Australia.
- Gaiotti, R. and Smith, B.S. (1992), “Stiffening of moment-resisting frame by precast concrete cladding”, *PCI J.*, **37**(5), 80-92.
- Ghosh, S.K. and Cleland, N. (2012), “Observations from the February 27, 2010, earthquake in Chile”, *PCI J.*, **57**(1), 52-75.
- Gjelvik, A. (1973), “Interaction between frames and precast panel walls”, *J. Struct. Div.*, ASCE, **100**(2), 405-426.
- Henry, R.M. and Roll, F. (1986), “Cladding-frame interaction”, *J. Struct. Eng.*, ASCE, **112**(4), 815-834.
- Hobelmann, J.P., Schachter, M. and Cooper, M.C. (2012), “Architectural precast concrete panel systems used for lateral-force resistance”, *PCI J.*, **57**(1), 124-134.
- Magliulo, G., Bellotti, D., Cimmino, M. and Nascimbene, R. (2018), “Modeling and seismic response analysis of RC precast Italian code-conforming buildings”, *J. Earthq. Eng.*, **22**(2), 140-167.
- Magliulo, G., Ercolino, M. and Manfredi, G. (2014a), “Influence of cladding panels on the first period of one-story precast buildings”, *Bull. Earthq. Eng.*, **13**(5), 1531-1555.
- Magliulo, G., Ercolino, M., Petrone, C., Coppola, O. and Manfredi, G. (2014b), “Emilia earthquake: the seismic performance of precast RC buildings”, *Earthq. Spectra*, **30**(2), 891-912.
- Metelli, G., Bettini, N. and Plizzari, G. (2011), “Experimental and numerical studies on the behaviour of concrete sandwich panels”, *Eur. J. Environ. Civil Eng.*, **15**(10), 1465-1481.
- Molina, F.J., Marazzi, F., Viaccoz, B. and Bosi, A. (2013), “Stability and accuracy in hybrid test example”, *Earthq. Eng. Struct. Dyn.*, **42**(3), 469-475.
- Negro, P. and Lamperti Tornaghi, M. (2017), “Seismic response of precast structures with vertical cladding panels: the SAFECCLADDING experimental campaign”, *Eng. Struct.*, **132**, 205-228.
- Negro, P., Bourmas, D.A. and Molina, F.J. (2013), “Pseudodynamic Tests on a full-scale 3-storey precast concrete building: global response”, *Eng. Struct.*, **57**, 594-608.
- Okazaki, T., Nakashima, M., Suita, K. and Matsumiya, T. (2007), “Interaction between cladding and structural frame observed in a full-scale steel building test”, *Earthq. Eng. Struct. Dyn.*, **36**(1), 35-53.
- Palsson, H., Goodno, B.J., Craig, J.I. and Will, K.M. (1984), “Cladding influence on dynamic response of tall buildings”, *Earthq. Eng. Struct. Dyn.*, **12**(2), 215-228.
- Pantoli, E., Hutchinson, T.C., McMullin, K.M., Underwood, G.A. and Hildebrand, M.J. (2016), “Seismic-drift-compatible design of architectural precast concrete cladding: tieback connections and corner joints”, *PCI J.*, **61**(4), 38-52.
- Pecce, M., Ceroni, F., Bibbò, F.A. and De Angelis, A. (2014), “Behaviour of RC buildings with large lightly reinforced walls along the perimeter”, *Eng. Struct.*, **73**, 39-53.
- Pinelli, J.P., Craig, J.I., Goodno, B.J. and Hsu, C.C. (1993), “Passive control of building response using energy dissipating cladding connections”, *Earthq. Spectra*, **9**(3), 529-546.
- Pinelli, J.P., Moore, C., Craig, J.I. and Goodno, B.J. (1992), “Experimental testing of ductile cladding connections for building façades”, *Struct. Des. Tall Spec. Build.*, **1**(1), 57-72.
- Pinelli, J.P., Moore, C., Craig, J.I. and Goodno, B.J. (1996), “Testing of energy dissipating cladding connections”, *Earthq. Eng. Struct. Dyn.*, **25**(2), 129-147.
- Psycharis, I.N., Kalyviotis, I.M. and Mouzakis, H.P. (2018), “Experimental investigation of the response of precast concrete cladding panels with integrated connections under monotonic and cyclic loading”, *Eng. Struct.*, **159**, 75-88.
- Sargin, M. and Handa, V.K. (1969), “A general formulation for the stress-strain properties of concrete”, *Solid Mech. Div.*, **3**, 1-27.
- Savoia, M., Buratti, N. and Vincenzi, L. (2017), “Damage and collapses in industrial precast buildings after the 2012 Emilia earthquake”, *Eng. Struct.*, **137**, 162-180.
- Scotta, R., De Stefani, L. and Vitaliani, R. (2015), “Passive control of precast building response using cladding panels as dissipative shear walls”, *Bull. Earthq. Eng.*, **13**, 3527-3552.
- Takeda, T., Sozen, M.A. and Nielsen, N.N. (1970), “Reinforced

- concrete response to simulated earthquakes”, *J. Struct. Div.*, ASCE, **96**(12), 2557-2573.
- Toniolo, G. and Colombo, A. (2012), “Precast concrete structures: the lesson learnt from L’Aquila earthquake”, *Struct. Concrete*, **13**(2), 73-83.
- Toniolo, G. and Dal Lago, B. (2017), “Conceptual design and full-scale experimentation of cladding panel connection systems of precast buildings”, *Earthq Eng. Struct. Dyn.*, **46**(14), 2565-2586.
- Wang, M.L. (1987), “Cladding performance on a full scale test frame”, *Earthq. Spectra*, **3**(1), 119-173.
- Yuksel, E., Karadoğan, F., Ozkaynak, H., Khajehdei, A., Güllü, A., Smyrou, E. and Bal, I.E. (2018), “Behaviour of steel cushions subjected to combined actions”, *Bull. Earthq. Eng.*, **16**(2), 707-729.
- Zoubek, B., Fischinger, M. and Isaković, T. (2016), “Cyclic response of hammer-head strap cladding-to-structure connections used in RC precast buildings”, *Eng. Struct.*, **119**, 135-148.
- Zoubek, B., Fischinger, M. and Isaković, T. (2018), “Seismic response of short restrainers used to protect cladding panels in RC precast buildings”, *J. Vib. Control*, **24**(4), 645-658.

HK